

A Thesis

entitled

Improvements in 3D breast treatment plan quality and efficiency through computer
automation of tangential breast radiotherapy treatment plans

by

Jacob Michael Gibbs

Submitted to the Graduate Faculty as partial fulfillment of the requirements for the

Master of Science Degree in

Medical Physics

Dr. Nicholas Sperling, Committee Chair

Dr. Sulaiman Aldoohan, Committee Member

Dr. David Pearson, Committee Member

Scott C. Molitor, Associate Dean
College of Graduate Studies

The University of Toledo

May 2023

© 2023 Jacob Michael Gibbs

This document is copyrighted material. Under copyright law, no parts of this document may be reproduced without the expressed permission of the author.

An Abstract of
Improvements in 3D breast treatment plan quality and efficiency through computer
automation

by

Jacob Michael Gibbs

Submitted to the Graduate Faculty as partial fulfillment of the requirements for the
Master of Science Degree in
Medical Physics

The University of Toledo
May 2023

Breast cancer is the most common type of cancer in women. More than 287,000 cases of aggressive breast cancer were estimated to have been diagnosed in 2022, leading to roughly 43,000 deaths. Breast radiotherapy has been shown through more than 50 years of clinical trials to be as effective as other treatments such as mastectomy. Clinical efficacy combined with frequent breast cancer diagnosis means that a significant amount of time will be spent by clinical staff planning breast radiotherapy treatments. If the process of treatment planning could be automated, then this same clinical staff would have more time to devote to other less routine cases. The aim of study is to design a script protocol to automate the process of beam segment design and machine output weighting, then to test this protocol against datasets of different geometries.

A beam segment generation and monitor unit (MU) weighting protocol was developed and designed within the RayStation treatment planning system (TPS) python software IDE. The design of the protocol is to take human designed open fields and create sub-fields, or segments (FiF – or Field-in-Field), to increase the homogeneity of

the radiation distribution. The protocol was tested on 10 CT datasets with five right side breast targets and five left side breast targets. Dose-volume statistics, dose distributions, and homogeneity index were calculated along with other plan parameters to test against recent published literature.

The study found an average homogeneity index of 0.10 across all 10 plans, and no hot spot above 107% when normalized to 95% of prescription dose to 95% of the target volume (or $D_{95}=95\%$). This normalization to the prescription dose level is the gold standard in clinical trials, including the Fast, Fast-Forward, and RTOG-1005 trials. The study also noted higher than expected out-of-field dose to the contralateral breast. The homogeneity of the radiation distribution of the plan is the only factor which was significantly affected via the running of the script protocol, and the dose to critical organs at risk (OARs) was dependent on the initial design of the open fields.

Finally, the automated breast treatment planning script performed similarly to the performance of other auto-breast planning scripts in published literature when using the $D_{95}=95\%$ normalization. However, the protocol does not currently generate acceptable plans at the normalization of 100% of prescription dose absorbed in 95% of the volume due to large volume hotspots. The development cycle of the script auto-breast planning script will continue until it can produce clinically acceptable plans at the hoped for normalization. The protocol should be generalizable to other sites that are typically treated with 3D-CRT. (3D conformal radiotherapy)

Soli Deo Gloria, the source of my strength.

Acknowledgements

Thank you to my advisor, Dr. Nicholas Sperling, for guiding me through the research process and for his timely insights which made this project possible. Thank you to my teacher and program director Dr. David Pearson for his advice along the way. Thank you also to my undergraduate research professor, Dr. Adam Phillips, for providing me with copious amounts of research experience so that I knew what to expect.

Table of Contents

Abstract.....	iii
Acknowledgements.....	vi
Table of Contents.....	vii
List of Tables	ix
List of Figures.....	xi
List of Abbreviations	xii
1 Introduction.....	1
1.1 Background.....	1
1.1.1 Tangential Field-in-Field (FIF) Technique.....	5
1.2 Pseudo-forward Planning Strategy	9
1.3 Historical Clinical Experience	10
2 Methods and Materials.....	12
2.1 Scripting.....	12
2.2 Segment Generation.....	14
2.2.1 Automated beam weighting.....	17
2.3 Clinical Goals	18
2.4 Optimization Criteria	19
2.5 Automation Evaluation Scale	19

2.6 Quantitative Description of the Dose Distribution	21
2.7 Organs at Risk Evaluation	23
2.8 Evaluation of SAP plans	25
3 Results and Discussion	26
3.1 Dose to Organs at Risk	26
3.2 Plan Parameters not related to Dose	33
3.3 Dose homogeneity	34
3.4 Automation grade	41
4 Conclusions.....	43
5 Future work.....	46
References.....	48
A.....	52

List of Tables

2-1: Automation Grading System.....	21
3-1: non-Dosimetric, plan-related parameters for the sample dataset.	33
3-2: Dose homogeneity using a $D_{95\%}=95\%$ normalization.	33
3-3: Dose homogeneity using a $D_{95\%}=100\%$ normalization.	35
3-4: Table of automation grade by dataset.....	41
A-1: Max point dose for left sided breast plans.....	52
A-2: Max point dose for right sided plans.	52
A-3: Mean Heart dose for left sided plans.....	53
A-4: Mean heart dose for right sided breast plans.	53
A-5: Volume of heart receiving 20 Gy in left sided breast plans	54
A-6: Volume of heart receiving 20 Gy in right sided breast plans	54
A-7: Volume of heart receiving 10 Gy in left sided breast plans.	55
A-8: Volume of heart receiving 10 Gy in Right sided breast plans.....	55
A-9: Max point dose to the Contralateral –Right—Breast in Left sided breast plans.....	56
A-10: Max point dose to the Contralateral –Left—Breast in Right sided breast plans.....	56

A-11: Volume at dose statistics for Ipsilateral –left-- Lung in left sided breast plans.....	57
A-12: Volume at dose statistics for Ipsilateral –Right-- Lung in Right sided breast plans.	57
A-13: Volume at dose tables for Ipsilateral –left—Lung in left sided breast plans when normalized to the literature standard of $D_{95\%}=95\%$	58
A-14: Volume at dose tables for Ipsilateral –left—Lung in left sided breast plans when normalized to the literature standard of $D_{95\%}=95\%$	58
A-15: Proportion of each dataset that received dose of 103%, 105%, and 107% for plans normalized to $D_{95\%}=95\%$	59
A-16: Proportion of each dataset that received dose of 103%, 105%, and 107% for plans normalized to $D_{95\%}/V100\%$	59
A-17: Homogeneity index values calculated using the $D_{50\%}$ as the denominator instead of the prescription.....	60

List of Figures

1-1: Beam arrangement for tangential breast radiotherapy.....	6
1-2: Beam arrangement for tangential breast radiotherapy.....	7
2-1: Script auto-planner (SAP) flowchart.	13
2-2: Isodose lines for control point design.....	15
2-3: Control point covering Near Isodose line.....	15
3-1: Maximum point dose of the target volume by site and normalization.	27
3-2: Mean heart dose by site and normalization.	30
3-3: Maximum dose delivered to the contralateral breast.....	30
3-4: Ipsilateral Lung Volume at 20% of Rx dose.	31
3-5: Ipsilateral lung volume at 10% of Rx Dose.....	31
3-6: Ipsilateral lung volume at 5% of Rx Dose.....	32
3-7: DVH curves for all left sided radiotherapy treatment sites.	37
3-8: DVH curves for all right sided radiotherapy treatment sites.	37
3-9: SAP developed radiation distribution for a left breast plan.	40
3-10: SAP developed radiation distribution for a right breast plan.	40

List of Abbreviations

3D-CRT.....	3D-Conformal radiotherapy
AAPM.....	American Association of Physicists in medicine
BEV.....	Beams eye view
cGy.....	Centi-Gray
CT.....	Computed tomography Volumetric Scan
D_{max}	Point of Maximum Dose
D_{mean}	Mean dose to a volume
DVH.....	Dose volume histogram
DX/VX.....	Dose (% of Rx)/V (% of target volume)
FIF.....	Field-In-Field
Gy.....	Gray
HI.....	Homogeneity index
IDE.....	integrated development environment
IMRT.....	Intensity Modulated Radiotherapy
LPO.....	Left posterior oblique
MLC.....	Multi-leaf collimator
MU.....	Monitor Unit
NSABP.....	National Surgical Adjuvant Breast and Bowel Project
OAR.....	Organ at Risk

ROI..... Region of Interest
RPO..... Right posterior oblique
RTOG..... Radiation Therapy Oncology Group
Rx..... Prescription dose level

SAPScript Automated planning system

TPS..... Treatment planning System

VMAT..... Volumetric Modulated Arc Therapy

Chapter 1

Introduction

1.1 Background

More than 287,000 cases of invasive breast cancer were estimated to have been diagnosed in 2022 in the United States, along with roughly 43,000 deaths [1] [2]. The use of radiation in conjunction with other therapies has been shown to be as effective as a radical mastectomy at controlling disease and preventing local cancer re-occurrence [3]. Recent studies have explored the possibility of reducing the length of the treatment course to just 5 fractions where a 5-6 week, 25-30 fraction course might once have been prescribed [4]. One can expect an increase in the number of patients seeking radiation to treat their breast cancer when the barrier of a multi-week daily treatment course significantly reduced. Therefore, it becomes necessary to find strategies to reduce the time expenditure of treatment planning and execution. The advent of treatment planning systems which use CT data to accurately calculate the dose that would be delivered by

the execution of a radiation therapy plan have opened significant new opportunities for the automation of a radiation therapy treatment planning via script automation and iterative optimization.

Radiation therapy is a treatment technique that uses radiation sources to shower a diseased region of the human body with photons or electrons. The radiation interacts primarily with electrons in the human body and deposits energy there. The energy is deposited in such a way that diseased (cancerous) cells are damaged more so than healthy cells, which can be utilized to treat many illnesses. The energy imparted to the body can be estimated, its unit of measure is the Gray which is the deposited energy per unit mass at a point (Joules/Kilogram) or (Energy/Mass of absorbing material).

In this study we consider three different strategies for radiotherapy treatment planning: 3D-conformal radiotherapy (3D-CRT), Intensity Modulated Radiation Therapy (IMRT), and Volumetric Modulated Arc Therapy (VMAT). The different strategies reflect differences in planning technique, levels of automation, and the need for patient specific quality assurance. In forward planned strategies such as 3D-CRT, the human planner defines the shape of each radiation field to be created via Multi-leaf Collimator (MLC) and defines a radiation output for that field. The gantry of the linear accelerator is stationary for each field, though it can be rotated in-between fields to achieve a more conformal dose distribution. This is only feasible for a few fields and requires the time

and expertise of the human planner to make an acceptable plan. IMRT is a more complicated version of 3D-CRT where MLCs are used to modulate the intensity of the beam to achieve a better dose distribution than 3D-CRT, computers which optimize field shape and intensity are used in a treatment planning technique called “inverse planning”. VMAT, in contrast to static field IMRT, is a form of IMRT where the gantry is in constant motion. Here gantry speed, dose-rate, and field shape are all optimized through inverse planning techniques to achieve the desired dose distribution.

The choice of treatment technique is highly patient anatomy dependent. There is evidence that IMRT inverse planning techniques decrease toxicities such as acute and chronic radiation pneumonitis and dermatitis; however, they also increase low dose spillage relative to 3D-CRT [5].

IMRT is a technique that hands total control of field shape and MU weightings to the iterative optimizer in hopes that the computer will deliver superior dose distributions. This can be done if enough sub-fields are added, at the expense of increased dose to the surrounding tissue. Further issues arise with the fact that the treatment field shapes are complicated and do not resemble human planned treatment techniques.

Parameters can be controlled through the optimizer. We can tell the optimizer to only find the best solution by optimizing beam weightings. This leaves our human-made control points alone, while finding the appropriate beam weightings to yield a

homogenous dose. This process would generally be done by a human in a similar iterative manner. Where higher MU's (Monitor units are a relative measure of the machines output, as measured by a monitor ionization chamber in the head of the linear accelerator) are gradually assigned to segments, with the dose being scaled each time until the segment lends sufficient coverage to the low dose region. As the computer is simply automating the same process that a human would use to come to the exact same solution as the human planner in a shorter amount of time, we argue that this technique would not be considered full IMRT, but a computer assisted 3D-CRT technique.

A second opportunity presents itself in the form of the open field. When the open field is defined in the treatment planning system, dose can be calculated. The machine output can then be scaled to show the required machine output to achieve desired coverage to the target volume. The dose appears to be very in-homogeneous, with areas of high and low dose present. This is either due to patient geometry or the presence of tissue inhomogeneities which change the rate at which radiation is absorbed. This information is then used by the planner (computer or human) to generate smaller fields which modulate beam intensity locally to create a more homogenous dose distribution. It stands to reason that the dose gradients present in the open field could be used to inform the creation of human-like control points in an automated fashion.

1.1.1 Tangential Field-in-Field (FIF) Technique

Both IMRT and 3D-CRT treatment planning techniques can utilize a method of beam arrangements where the beam isocenter is placed near the chest wall of the patient, or just barely inside the ipsilateral lung [6]. Two parallel-opposed beams are generated about the isocenter at oblique angles; one superior and one inferior to the patient as in Figure 1-1 [7]. This shows an Axial CT image with the typical arrangement of parallel opposed beams in the tangential field technique. The proximal half of each beam is close off to the isocenter with MLCs to reduce collateral dose to organs at risk (OAR's). The proximal Jaws and MLCs are moved to the Isocenter to prevent beam divergence into ipsilateral lung or heart. Care is taken to shield the humerus with MLCs and to allow the distal Jaw and MLCs significant margin.

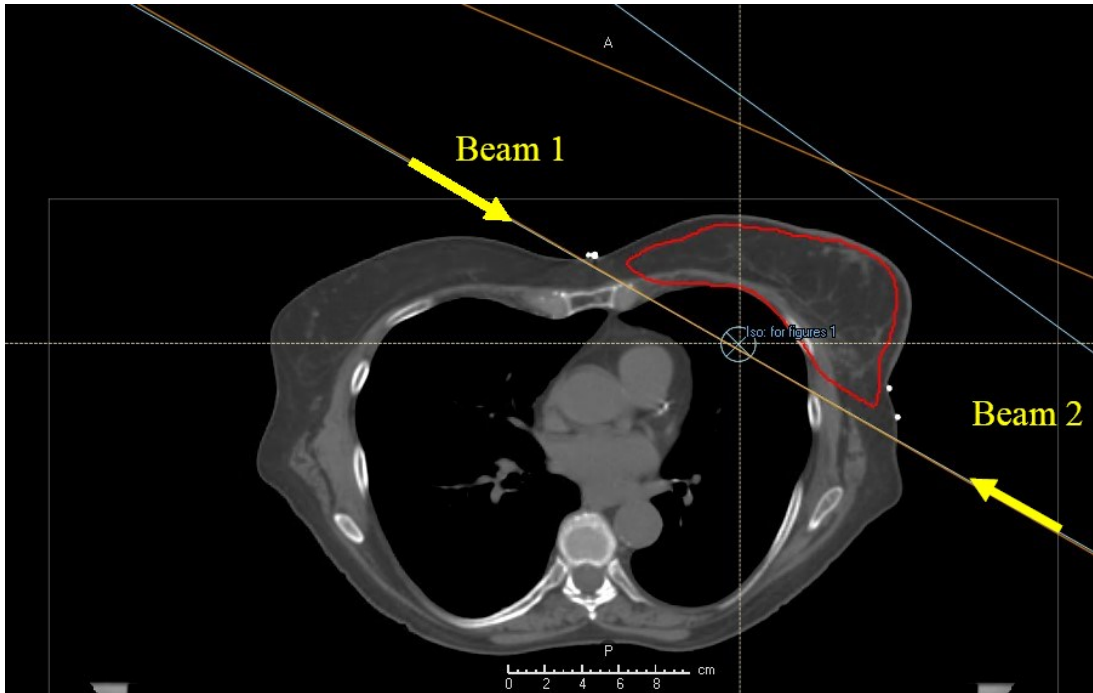


Figure 1-1: Beam arrangement for tangential breast radiotherapy.

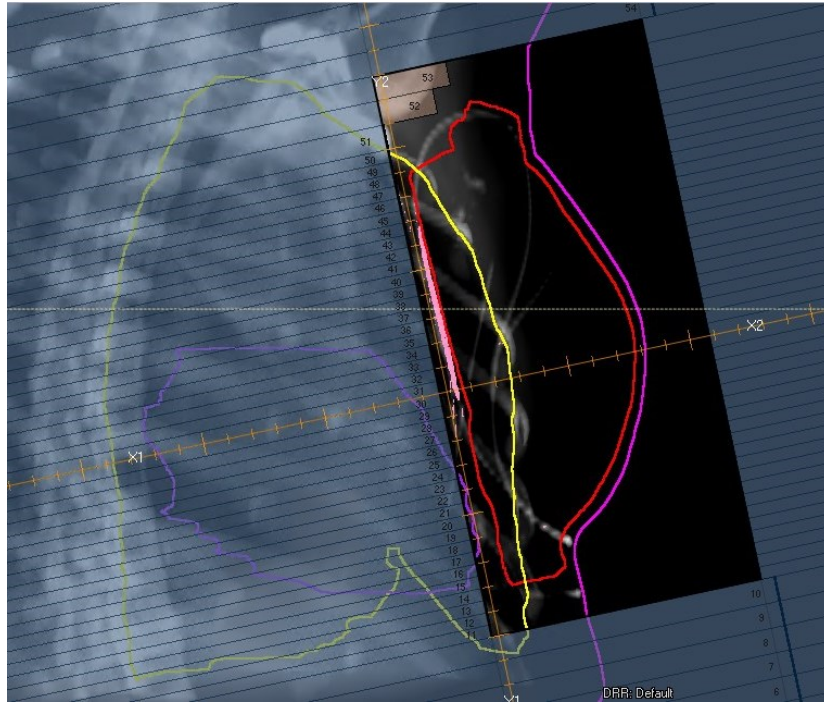


Figure 1-2: Beam arrangement for tangential breast radiotherapy.

The field-in-field technique is a way of describing the process of starting with an open field that roughly conforms to the target volume in the BEV, then creating smaller sub-fields –also named beamlets or segments-- which increase the delivered fluence to sub-regions of the target volume. This is used to shield regions of tissue that would otherwise absorb too much dose from the open field (blocks). In the case of Breast radiotherapy planning, the distal regions of the breast away from the chest wall are significantly thinner than the proximal chest wall region. They must be shielded by MLCs from receiving the full open-field dose. This is typically called tissue compensation because the MLCs are acting like missing tissue.

The increase in fluence to low dose regions allows the open field output to be decreased, while achieving the same coverage as the initial dose distribution, which has the effect of decreasing the dose delivered to high dose regions and an overall increase in field uniformity. This process can be carried out iteratively for as many entrance directions as is desirable, with an increasing number of open-field beams comes greater field conformity and an increase in low dose to normal tissue. The typical beam weighting is about 20% on the segments and 80% on the open field, though this is highly dependent on the particulars of the patient anatomy.

1.2 Pseudo-forward Planning Strategy

To appropriately inform the creation of segments via the FiF technique, the magnitude of tissue compensation must be assessed for each location relative to the aperture. The treatment machine must solve a problem created in three dimensions, with a 2-dimensional tool, the MLC collimator system. The segment shape must be created which yields a homogeneous dose distribution in all three dimensions. The necessary information can be gained by applying monitor units to the open fields, calculating the dose imparted to the tissue, and normalizing the open field. The dose gradients caused by geometry and tissue inhomogeneities can then be visualized and compensated.

The best method of calculation for each isodose level will depend on the initial method of dose normalization. Isodose levels could be specified via a percentage of the prescription dose level, but the amount of work each control point would have to do would dramatically increase as the prescription would increase. If the breast prescription was 5000 cGy, then the 105% isodose line would be at 5250, and each control point might be responsible for smoothing 250 cGy of dose gradient. Whereas a 4000 cGy prescription would require each control point to smooth out only 200 Gy of dose gradient. This would exacerbate the “dose plateau” effect in plans with high dose gradients and would decrease overall dose uniformity.

Another method of creating isodose levels would be to choose the level of dose gradient that each control point is required to mediate, the number could be set at 150 cGy of dose deviation from prescription. This method would work most effectively if the dose gradient to be mediated was the dose difference between the maximum dose of the distribution when the dose created by the open field blocks are scaled to meet prescription and the 105% dose level of prescription. The final method would be to only scale the open fields until the max dose was equal to the prescription dose level, then each control point could add fluence to the areas that still lack prescription coverage. This method might require each control point to be added individually, scaling after the creation of each control point to keep the maximum point dose at an acceptable level.

1.3 Historical Clinical Experience

The Fischer trial (NSABP-b04) [3] is an excellent example of an early trial of whole breast radiotherapy which yielded the result that breast radiotherapy was just as effective as a radical mastectomy in the sense that they had roughly equivalent disease-free survival and hazard ratios [3]. A hazard ratio is defined as the ratio of a person's probability of receiving experiencing effect with or without an intervention, such as the intervention and control arms of a randomized controlled trial. The trial popularized the standard 50 Gy in 25 fractions, or the standard fractionation. This trial was published in 1974, so it has nearly 50 years to accumulate long-term data and acceptance.

However early clinical trials all pre-dated the widespread use of 3D-CRT. Or the use of CT scans and Organ contouring software to obtain accurate dose statistics for volume regions of the human body. Even the UK fast trial protocol had no minimum standards for heart dose or ipsilateral lung dose [8]. The IMPORT-HIGH trial and Fast-Forward trials [4] all had dose volume statistics for heart and lung doses, but the most comprehensive clinical trial protocol resulted from NRG's RTOG 1005 [9] clinical trial which contains comprehensive dose-volume statistics. The RTOG protocol will be considered the minimum standard of acceptability because it is new enough to have a comprehensive dose constraint table for both the target volume and for OARs. While also having about 8 years of long-term data to support the efficacy of the radiotherapy plans that were enrolled in the clinical trial [10].

Chapter 2

Methods and Materials

2.1 Scripting

The RayStation (Raystation Laboratories, Stockholm) Treatment Planning System (TPS) contains within it a scripting environment (Integrated development environment) which includes custom libraries for integration into, and automation of, the planning system. CPython 3.8 was chosen for the development of this program [11]. In keeping with the stated aim of the study, the following method is designed to automate the process of segmentation and segment weighting to optimize the dose homogeneity of the tangential multi-segment breast radiotherapy plan with the protocol shown in Figure 2-1. The program is designed to operate without human planning intervention from the point of human block creation. Human derived blocks are required because human geometry can vary significantly, and ideal Isocenter and beam angle can require clinical judgement.

Methods have previously been developed to obtain the correct beam angle, but do not address issues such as lung and heart sparing [12].

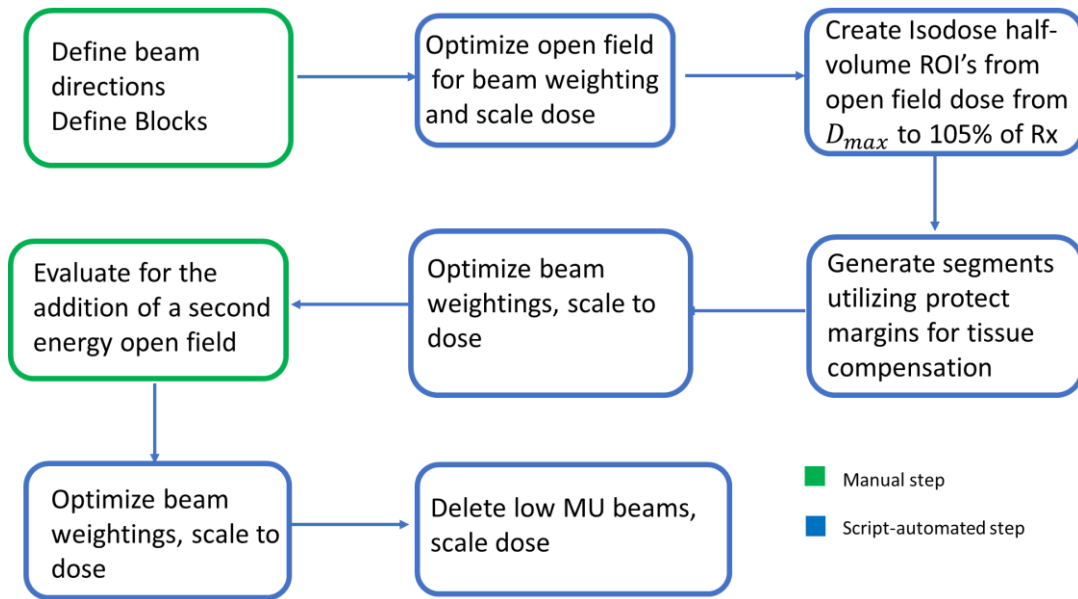


Figure 2-1: Script auto-planner (SAP) flowchart.

2.2 Segment Generation

The basic method of tissue compensation is to apply machine output (MU's or monitor units) to the open, parallel-opposed fields until the dose prescription is met for the PTV volume. This ensures that the beam is outputting sufficient fluence to impart prescription dose to the entire target volume. Areas with less tissue thickness will be covered with very high doses, while thicker regions will necessarily experience "just enough" dose to meet prescription. ROIs are then created at even dose levels between dose-max and prescription. Figure 2-2 shows the isodose lines which are created from the open fields of the Blocks. The SAP creates a dummy beam orthogonal to the tangents and half-beam blocked on the medial edge. This beam is used to create a dose which may be turned into an ROI bisecting the breast at the isocenter. The ROI algebra tool is then used to assign each half of the field to the beam which enters on this side.

The dose gradient between each ROI from dose directly characterizes the amount of work that control point is expected to do in smoothing out the dose gradient. However, the curvature of the breast around the chest wall causes some cold spots to be "shielded" by hot spots closer to the beam aperture.

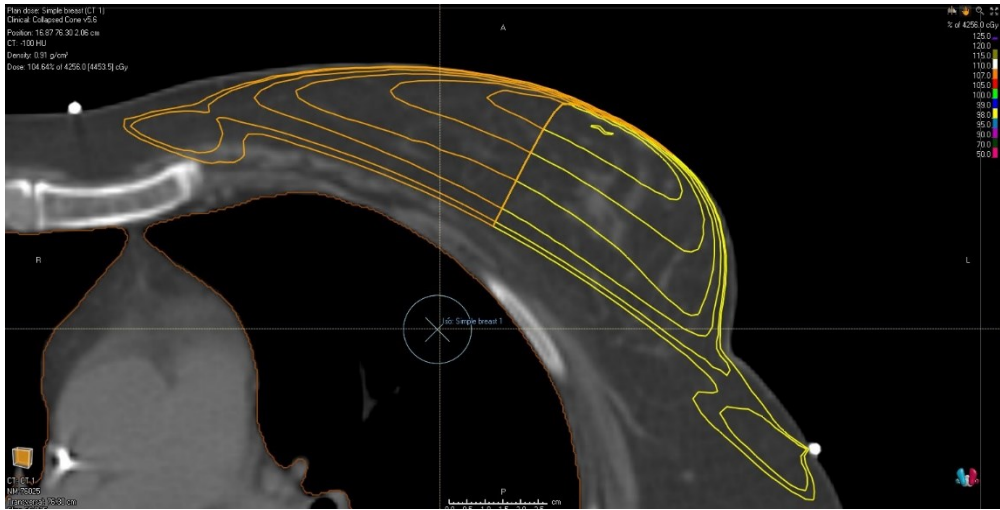


Figure 2-2: Isodose lines for control point design

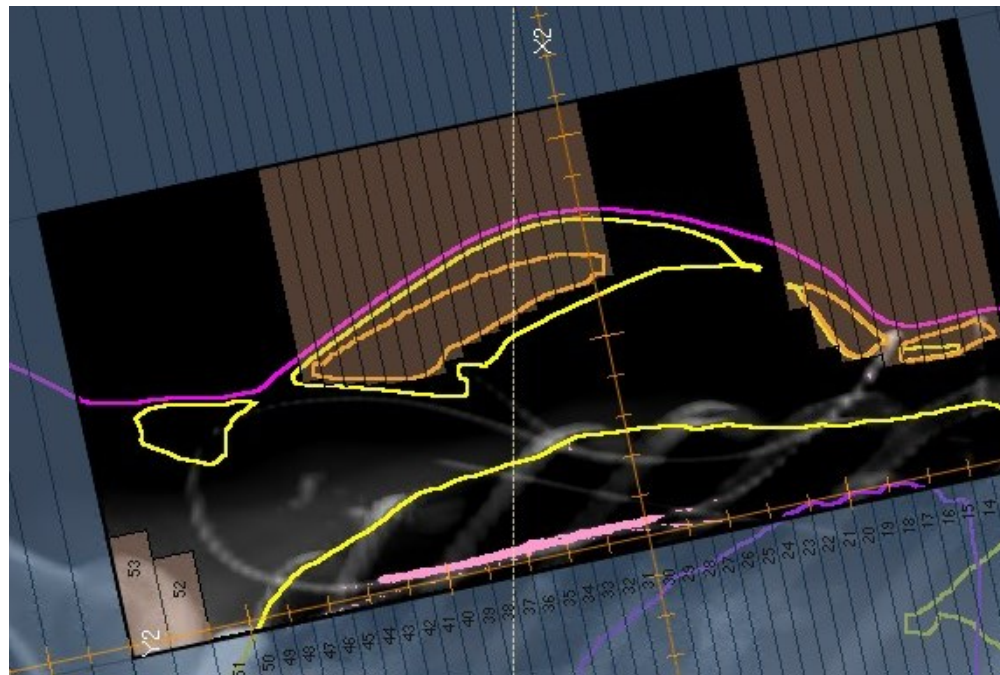


Figure 2-3: Control point covering Near Isodose line.

Each open field is then copied once per dose-ROI. Protect margins were assigned to the near dose-ROI for each beamlet in the parallel opposed arrangement. This allows the greatest contributor to the dose in that region to do most of the tissue compensation. The aperture shape of each beamlet is conformed by moving the closest MLCs to cover the assigned near dose-ROI. Figure 2-3 shows the resultant control point which is assigned to the LPO Block. Also shown near the bottom of the figure is the left lung in yellow and the heart in purple. The orange and yellow isodose volumes are of the same isodose level. Beam segment conforming to the near-isodose volume to avoid screening by the far isodose volume of the same dose level.

The standard FiF method is to only use the distal bank of MLCs to compensate because the distal portion of the breast has the least tissue and requires the most tissue compensation. To ensure that distal MLCs are always closest to the dose ROI's, the medial MLC bank is temporarily moved as far from the patient as possible (19 cm, the absolute Max is 20 cm on the Varian Truebeam linear accelerator). This provides the fundamental maximum patient dimension for which my code could be used at a Max target width of 20 cm scaled to be measured in the beams eye, at the MLC bank. The current function limit is 15 cm at the location due to the maximum leaf position differential, this is machine specific.

2.2.1 Automated beam weighting

The human derived block defines the absolute maximum extent of the human body that is exposed to open field radiation and is affected by that target treatment volume. Optimization goals are then created which focus on uniform dose and coverage. The optimizer will focus on increasing dose uniformity via beam weighting. Asymmetric tissue distribution necessitates asymmetric weighting because thicker tissue will require a higher beam weighting to maintain adequate coverage. The MU values are then scaled on each beam to the specified normalization, and isodose volumes are created along the dose gradient at specified dose levels.

Each isodose volume represents a new area that is to be covered by MLCs using the “Protect Margin” feature in the RayStation TPS which directs a beam to cover a volume with MLCs in the linear accelerator’s beams eye view “BEV”.

The monitor unit is an arbitrary unit which corresponds to the amount of Ionization detected by the monitor chamber of the linear accelerator. This is directly related to the amount of dose delivered by the linear accelerator via the method Described in AAPM TG-51 through clinical reference dosimetry. [13] At our facility, 1 Monitor Unit (MU) is set to 1 cGy under the reference conditions of a 10x10cm² field, at 100 SSD (the distance between the target and the surface of the attenuating medium), and 10 cm depth in a minimum square water tank of 30 cm on a side. The modulation factor is a

consequence of the fact that segments shield parts of the beam, requiring more machine output to achieve the same dose per fraction.

We can quantify the relative extent that a radiation plan relies on its smaller sub-fields (beam segments) by calculating the modulation factor (Mod Factor). This factor is defined as the quotient of the total Number of MUs/fx and the delivered dose/fx.

$$\text{Mod Factor} = \frac{\text{Delivered monitor units per fraction}}{\text{Dose delivered per fraction}}$$

2.3 Clinical Goals

Relevant plan quality parameters were chosen from a review of phase 3 clinical trials that have informed the breast treatments that are commonly prescribed at our clinic. This includes the international standard fractionation (popularized by the Fischer trial [3]), accelerated fractionation (RTOG-1005 [9]), and hypo-fractionated whole breast radiotherapy (Fast-forward trial [4]). Each trial specified minimum plan requirements. The most recent clinical trials include requirements for 3D-planning on a CT, which allows for organ contouring and the calculation of dose statistics over the resultant volumes.

2.4 Optimization Criteria

The built in RayStation iterative optimizer was utilized to modulate the output (MUs) to each segment and the open field. The optimizer was prevented from changing beam parameters such as aperture shape, field wedging, and beam direction. The optimizer works to obtain the most acceptable outcome through iterative optimization. The mechanics of which are beyond the scope of this paper.

2.5 Automation Evaluation Scale

The amount of time that the automated planning script saves is entirely dependent on its ability to create a clinically acceptable dose distribution without human intervention. Each improvement requires intervention that the planner must make costs time.

The main task of the automated script is to create appropriate control points and weigh them properly to create the most homogeneous distribution possible. Control points are intended to compensate for a lack of tissue, smoothing out the dose gradient that exists orthogonal to beam direction. However, sometimes that dose gradient is screened near the chest wall by a buildup of dose owing to the increase in depth. Beam segments like these may need to be adjusted. Other times some control points may become long and thin near the chest wall, applying a significant amount of monitor units

to increase fluence outside of the PTV, these control points must be deleted because they buildup large amounts of fluence near to ipsilateral lung and heart, so intrafraction motion could expose critical organs at risk to large amounts of radiation.

Huang et al. [14] created an automation grading system which grades patients on a 1 to 5 scale in their 2022 paper on automated whole-brain automated radiotherapy treatment planning where a grade 5 plan required no human intervention, and a grade 1 plan was not usable. This type of system produces a quick metric for script performance. The automation grading system uses an opposite numbering system, where grade 1 requires no human intervention and grade 5 is not usable.

This system was augmented to provide for the specific types of changes that might need to be made when working on tangential whole-breast radiotherapy. The automation grade is a method for describing the effectiveness by which the Automated breast planning script achieves a clinically acceptable plan beyond normal human interaction with the script.

Table 2-1: Adapted Automation Grading System

Automation grade	
1	Clinically acceptable plan with no human intervention required
2	clinically acceptable plan with less than 3 un-necessary changes per beam direction
3	less than 3 necessary changes per beam direction required to achieve a clinically acceptable plan
4	Several adaptations of aperture shapes required to achieve a clinically acceptable plan
5	clinically acceptable plan not attainable without significant human intervention

2.6 Quantitative Description of the Dose Distribution

The primary goal of the Script Automated Planner (SAP) is to create a homogeneous dose distribution. Therefore the primary dose statistics should relate to the dose distributions adherence to the prescription and normalization, and the homogeneity of the dose distribution. Therefore, the primary metrics we consider are minimum dose covering some percentage of the target volume, D_{mean} , D_{max} , HI, and volumes at fixed relative doses above prescription (Rx) (103%, 105%, and 107%).

The mean dose (D_{mean}) is the average dose when considering voxel doses calculated across the target volume. This is averaged on a per voxel basis and extracted as a part of the code. The maximum dose (D_{max}) is defined as the high dose level which is absorbed by a volume of at least $.01\text{cm}^3$. This was chosen as the smallest value which

could be set with certainty of the volume being specified. This is extracted with the OARs dose-volume statistics.

Isodose volumes at a dose level were specified in Mitchell et al. at 103%, 105%, 107% [15]. These definitions were used due to the similarities in the Mitchell auto-planner to the current study, the dose level statistics were calculated from the plan DVH curve and function to specify the size and magnitude of the plan hot spot [15].

The homogeneity index (HI) is a dose level resistant description of dose homogeneity for a radiation plan dose-volume histogram. It functions as a single quantitative assessment of dose adherence across the volume, and therefore is an important plan quality indicator for breast radiotherapy. Further discussion can be found in chapter 3.3. The definition used in this study follows was advocated for by Kataria et al. and is used in Mitchell et. al. so the HI will be directly comparable [16] [15].

$$HI = \frac{D_{98}-D_{02}}{D_{50}}$$

Where D_{98} is the maximum dose level absorbed by 98% of the target volume and D_{02} is the maximum dose level absorbed by only 2% of the target volume. D_{50} is the maximum dose absorbed by 50% of the target volume. The ideal value for the HI is zero, which would describe a “shoulder of zero width”, which essentially means that the entire target volume has the same dose value.

Where ranges are given for mean statistics, the format will be mean follow by the range of one standard deviation from the mean high and low of it. Values that approach zero will not display negative values in the mean if a negative value has no physical meaning.

2.7 Organs at Risk Evaluation

The RTOG 1005 [10] protocol sets comprehensive minimum dose statistics for organs at risk because it was designed for 3D radiotherapy with dose statistics being calculated for organs that are contoured on to the treatment planning CT [9]. This requires only that beam directions and apertures be defined, and dose calculated and normalized to the prescription. The aim of this section is to determine whether the auto-planner creates dose distributions that would be acceptable to relevant clinical trials for which we have long term data. This is a basic form of clinical acceptability that allows for data comparison to other literature such as Mitchell et al. and Archibald-Heeren et al [15] [12].

The doses to be evaluated for each plan will include those structures deemed critical based on the previously mentioned clinical trials and will include: the volume of the heart contour that receives 20 Gy (heart V_{20}), the volume of the heart contour that receives 10 Gy (V_{10}), the mean heart dose (heart D_{mean}). The mean heart dose is a good single indicator for the effect of treatment proximity to the heart. Heart dose should be

minimized because it can lead to the long-term morbidity of radiation related heart disease. RTOG recommends the following constraints on mean heart dose: maximum acceptable dose constraint is 500 cGy and the RTOG ideal constraint is 400 cGy. The heart is typically shielded as part of the blocks, and therefore out of field. This means that the heart dose can be kept low. However, a build-up of high MU segments near the heart region could increase the mean heart dose through scatter [10].

The maximum point dose of a plan is the maximum dose delivered to at least 0.01cm³ to the Target volume. The volume of the Max point dose was not defined in relevant literature. The maximum point dose should be as close to the prescription (Rx) dose level as possible. The maximum point dose is an indicator of the homogeneity of the radiation distribution across the breast, which is the overall goal of the SAP. The homogeneity of the radiation dose distribution across the breast has been linked to the cosmetic outcome of the breast, especially for increases in dose [17].

The purpose of lung objectives are to preserve basic lung function and to guard against acute and late forms of Radiation Pneumonitis [17]. As per RTOG 1005 protocol (Appendix VII), these set maximum volume sizes which can absorb a set dose level and vary by [9] Three volume constraints exist for 3 different dose levels of the Ipsilateral lung, which absorbs the most dose due to proximity to target. Each dose level may be absorbed by a maximum ipsilateral lung contour volume. Which means a maximum

volume (in % of the total volume) of that organs contour may absorb a maximum dose level (in cGy, this is not prescription dependent because the primary endpoint is lung function for the constraint). The contralateral lung is more distal to the target, and therefore only needs one maximum dose level at maximum volume constraint.

2.8 Evaluation of SAP plans

The Script automated breast planner was run on 5 CT datasets intended to simulate real world treatments: using right breast and left breast targets for 2 plans per dataset. The goal of the study is to determine the quality of the SAP produced dose distributions and segment quality. Segment quality and dose distribution quality are assessed in the automation score, which beam quality parameters only interrogate the dose distribution. The datasets were prepared with organs-at-risk (OARs) contours, and two blocks for half-beam blocked and parallel opposed beams.

Chapter 3

Results and Discussion

3.1 Dose to Organs at Risk

The evaluation of the plans run on each of the sample datasets are presented below. The scripted protocol was run more than once to determine the optimal set of beam energies as needed. Dose statistics were added, calculated, and exported via the script to ensure data consistency. What follows is a comprehensive list of statistics for the dose distributions of the 10 auto-generated breast plans for which plans were created.

While the ipsilateral breast is considered a target structure, it nevertheless has maximal dose constraints to consider. Figure 3-1 shows the maximum point dose to the Target volume, defined as the maximum dose which is absorbed by 0.01 cm³ volume. The maximum point dose is sorted by coverage normalization and site, and the value by plan can be found in Appendix A-1 and A-2.

V_{10} and V_{20} can be found in Appendix A, Tables A-5 – A-8, and approaches zero in all cases. Individualized plan data can also be found in Appendix A. The low values

are a result of the way blocks are set up (The Heart is shielded by MLCs in the beams eye view) and is not an indication of SAP effectiveness.

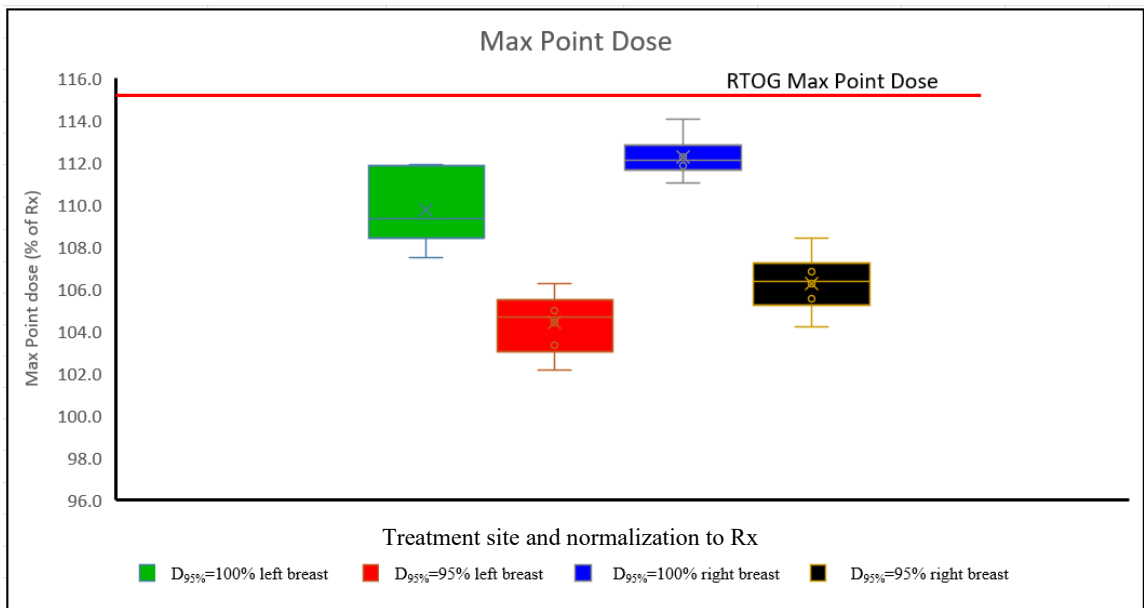


Figure 3-1: Maximum point dose of the target volume by site and normalization.

When evaluating mean heart dose, SAP has no part in controlling heart dose because good blocks will shield the heart before the script is run. It is the responsibility of the planner to control heart dose through beam direction and Block design. The evaluation of mean heart dose is presented in Figure 3-2. As can be seen, the mean heart dose achieved in the sample dataset is well below the constraints specified in the RTOG 1005 trial [9]: the RTOG protocol maximum acceptable dose constraint is 500 cGy and the RTOG ideal constraint is 400 cGy, which are off the scale and therefore not displayed.

Contralateral breast dose should be minimized to reduce the likelihood of radiation-induced cancer. Once again, much of the work is done with cleverly chosen beam direction and block choice. Contralateral breast dose failed or was close to failing in all right breasted cases based on the criteria selected for this study. Figure 3-3 shows the distribution of the maximum dose delivered to the contralateral breast for the selected plans. The cause of this out-of-field dose is a product of initial block design and potentially planning system and machine model and is therefore beyond the scope of this study.

The target volume often directly abuts the ipsilateral lung and may even curl around its outside edge. This has the effect of placing a portion of the lung directly in the path of the beam. Therefore it is important to pay attention to the dose levels which are

delivered to the ipsilateral lung because radiation exposure is associated with the development of acute, and then chronic pneumonitis [17]. While most of the work in shielding the lung is carried out via block design, the method of tissue compensation will inevitably increase dose to the medial beam edge. This is the edge that will irradiate the most ipsilateral lung tissue. The cost of homogeneous dose will be slightly more lung dose.

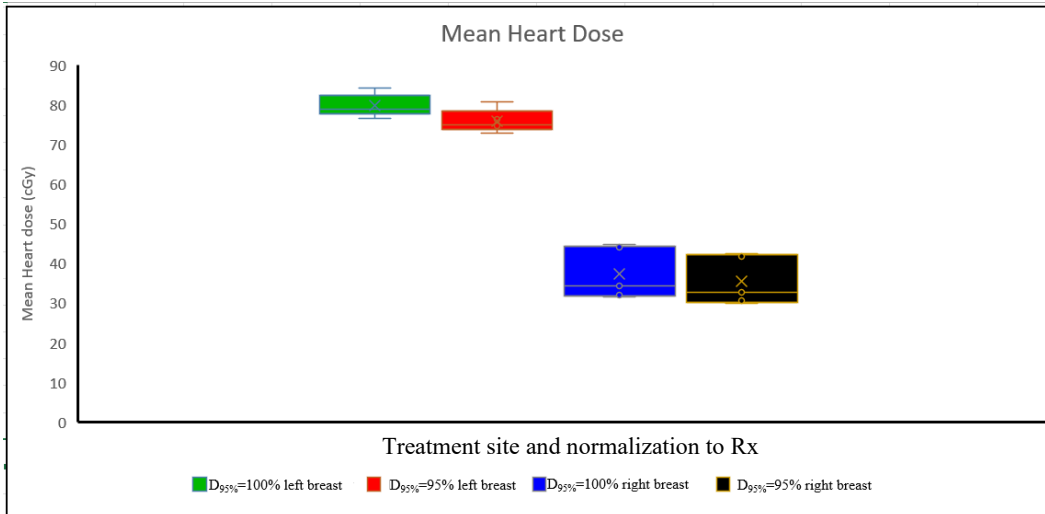


Figure 3-2: Mean heart dose by site and normalization.

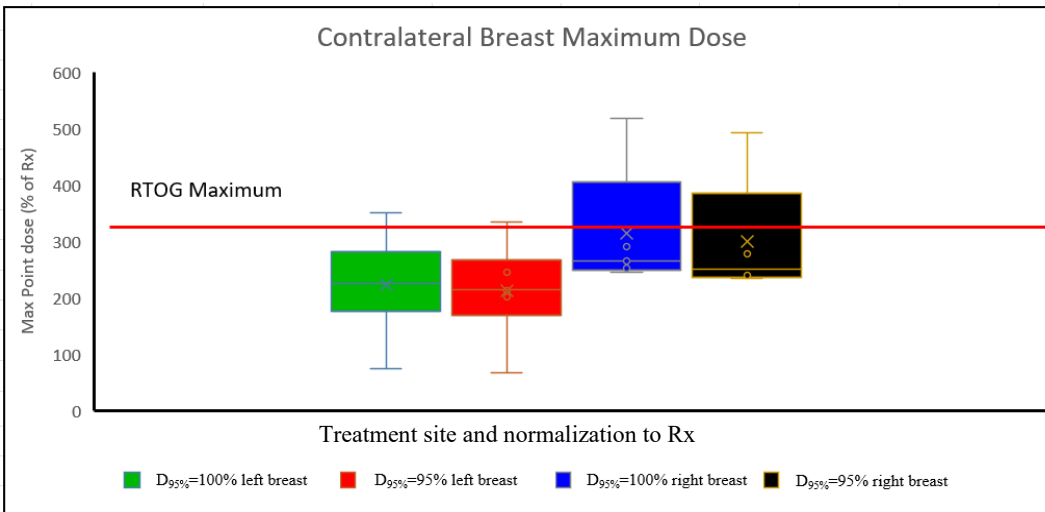


Figure 3-3: Maximum dose delivered to the contralateral breast.

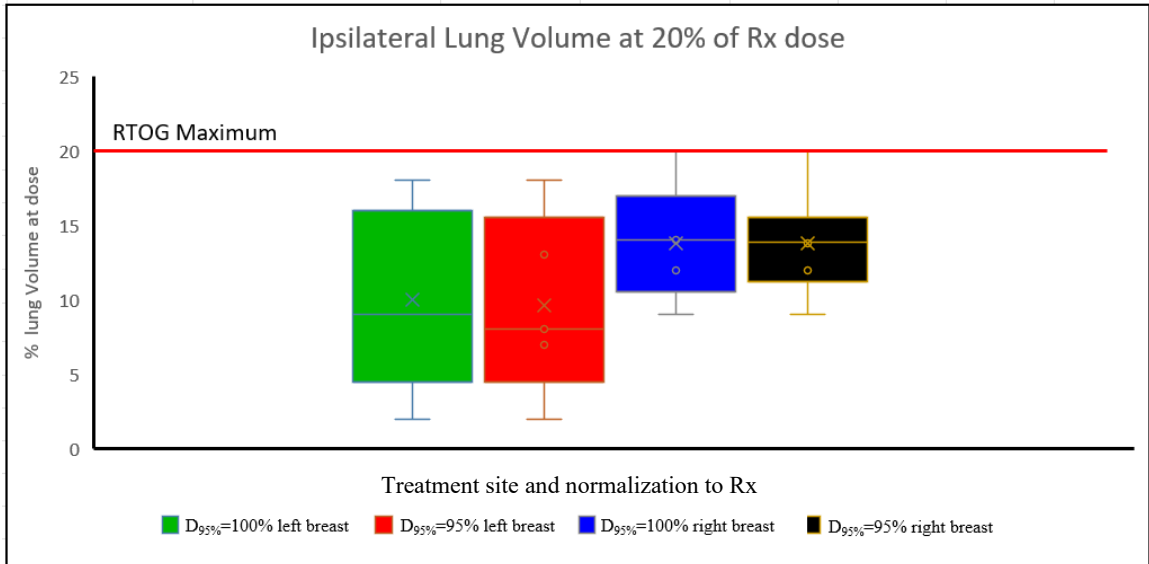


Figure 3-4: Ipsilateral Lung Volume at 20% of Rx dose.

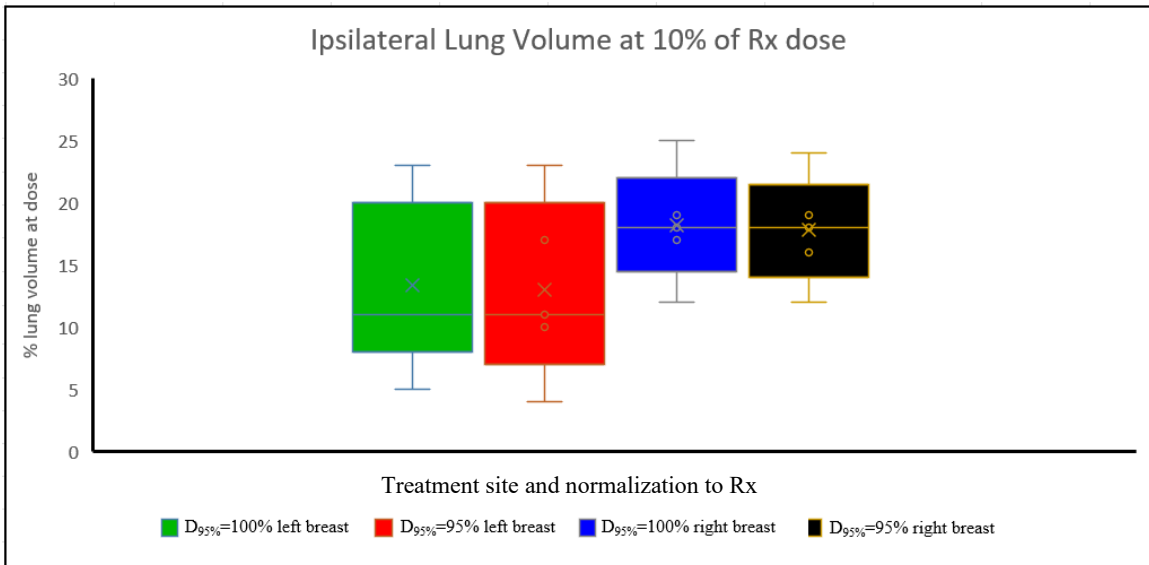


Figure 3-5: Ipsilateral lung volume at 10% of Rx Dose.

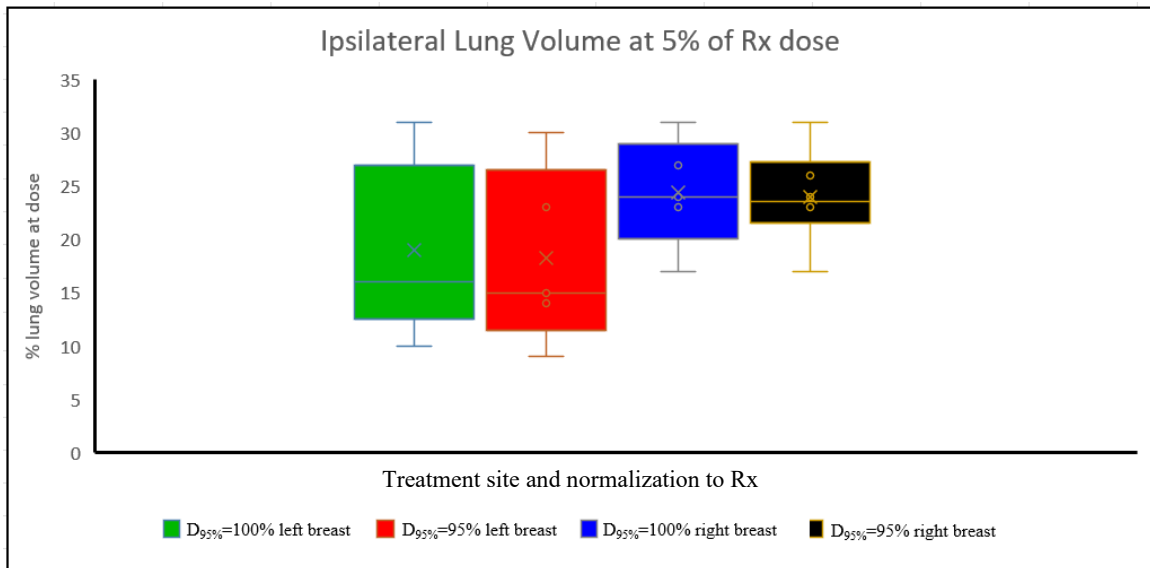


Figure 3-6: Ipsilateral lung volume at 5% of Rx Dose.

3.2 Plan Parameters not related to Dose

Table 3-1: non-Dosimetric, plan-related parameters for the sample dataset.

Dataset	# of MU/fx	Total CPs	Dose/fx	Modulation factor
dataset 1R	325.2	5	266	1.22
dataset 2L	365.4	11	266	1.37
dataset 3L	339.8	8	266	1.27
dataset 4R	314.4	16	266	1.18
dataset 5L	330.4	4	266	1.24
dataset 6R	313.2	4	266	1.17
dataset 7L	310.5	10	266	1.16
dataset 8R	297.9	3	266	1.11
dataset 9L	308.9	3	266	1.16
dataset 10R	320.5	7	266	1.20
Average	322.62	7.1	266	1.21

Table 3-2: Dose homogeneity using a $D_{95\%}=95\%$ normalization.

Target dose metrics ($D_{95\%}=95\%$)	Mean (range)		Mitchell et al. (2017)	
Coverage (at 95% of Rx dose)	95.1	(94.9 - 95.4)	95.4	(88.1 - 99.1)
D_max (% of Rx)	105.3	(102.7 - 106.0)	106.5	(104.8 - 108.0)
D_mean (% of Rx)	99.7	(4179 - 4241)	100.8	(98.5 - 102.0)
HI	0.10	(0.08 - 0.12)	0.11	(0.09 - 0.28)
V_103% (%)	4.51	(3.21 - 5.82)	11.8	(5.2 - 28.9)
V_105% (%)	0.37	(0.0 - 2.01)	0.6	(0.0 - 4.9)
V_107% (%)	0.00	(0.0 - 0.0)	0.0	(0.0 - 0.4)

3.3 Dose homogeneity

The main contribution of SAP to plan quality is to create the most homogeneous distribution possible. The tissue compensation method of creating beam segments attempts to solve dose gradients stemming from the extreme variation in tissue thickness within the breast. Therefore several methods are used to describe the homogeneity of the distribution of radiation created by the breast auto-planner.

The results in Table 3.2 show that the dose homogeneity using the $D_{95\%}=95\%$ normalization is comparable to that of published literature, shown compared with the Mitchell et al. dataset (n=40) to as a benchmark [15]. It accomplished this by using a similar mechanism to the Breast auto-planner Mitchell et. al. That the Mitchell Breast auto-planner was scripted in Pinnacle and the SAP was scripted in RayStation or the fact that the beam weighting technique of the SAP is automated appear not to affect the homogeneity of the dose distribution with respect to DVH statistics. Since the HI is essentially a numerical representation of the steepest gradient of the dose-volume histogram (DVH), the DVH curve is provided in Figure 3-7.

The most important and impactful functionality that SAP can have is on the dose homogeneity. A clinically acceptable auto-planner must be able to make reasonable human looking segments, and then also use those segments to create clinically acceptable dose distribution with minimal remaining dose gradients. However, the parallel dose

gradient caused by beam attenuation is still an issue that the SAP has some trouble resolving. Figure 3.1 shows one of the more ideally shaped dose distributions where there is still a significant surface hot spot. This hot spot exists because the beam weightings are optimized for coverage on the interior of the medial line. The beam intensity of the last 2 segments is increased until the center was sufficiently covered, however this leaves the surface of the dataset to absorb higher than prescription dose levels because it is exposed to the un-attenuated fluence of the beam. With the fluence being defined as the total particles per unit area resulting from machine output. This weakness, if not fixed before the script was clinically accepted could lead to higher risk of patient acute and long-term morbidity as described in the introduction of this study [6].

Table 3-3: Dose homogeneity using a $D_{95\%}=100\%$ normalization.

Dose homogeneity for all plans ($D_{95\%}=100\%$)	Mean (C.I.)	Mitchell et al. (2017)
Coverage (at 100% of Rx dose)	95.1 (94.9-95.4)	--
D_max (% of Rx)	111.02 (109.5-112.6)	--
D_mean (% of Rx)	104.09 (4395.2-4464.7)	--
HI	0.10 (.08-.12)	--
V_103% (% of target volume)	70.22 (70.0-70.4)	--
V_105% (% of target volume)	34.50 (33.7-35.3)	--
V_107% (% of target volume)	17.87 (16.5-19.3)	--

Table 3-3 shows the same homogeneity analysis as before with the dose scaled to $D_{95\%}=100\%$ to the target volume. The HI is numerically the same which is an expression of how the shape of the should does not change in a DVH during scaling, the whole shape is simply shifted laterally in the direction of increasing or decrease dose depending on the direction of the scaling. We can accept this without question because the aperture shapes and relative MU weighting is not changing, the dose at each point in the dataset simulation receives a dose that is perfectly linearly proportional to the delivered MU's with the modulation factor as the proportionality between MU and absorbed dose. This is also what allows us to conclude that this will work for all prescriptions, because the dose would simply be scaled without the need to re-optimize for block setup. However, the dose level specific benchmarks with respect to the set prescription of 4270 cGy do not stay the same, we can see that SAP plans normalized to $D_{95\%}=100\%$ would be seen as not homogeneous enough. This conclusion is reached by assume the minimum coverage describes the overall floor of the radiation distribution, D_{mean} describing the overall adherence to the prescription of all points in the target volume, the clinically significant value is the volume of target exceeding a 107% dose and D_{max} since those values have been link to poor cosmetic outcome, especially with the hotspots near the surface. With 17% of the target exceeding an absorbed dose of 107% of prescription. These plans on average would not be considered clinically acceptable at this normalization.

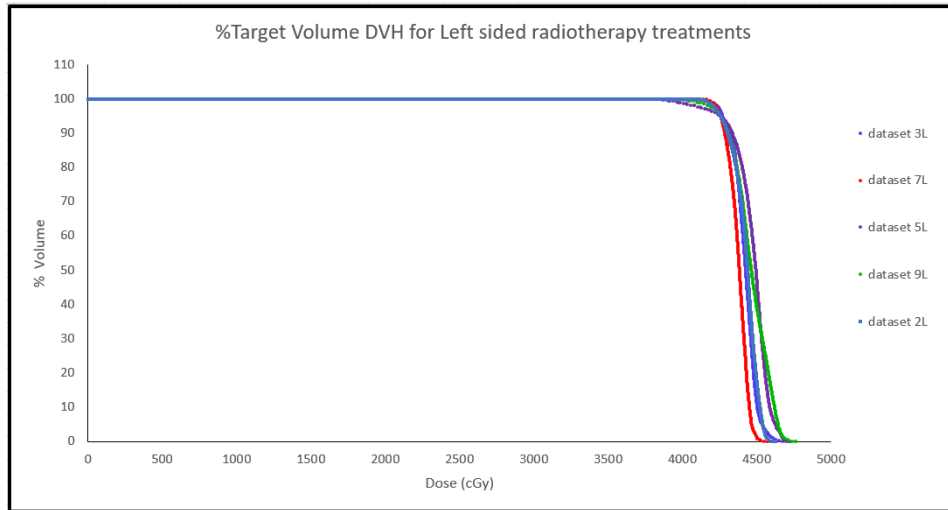


Figure 3-7: DVH curves for all left sided radiotherapy treatment sites.

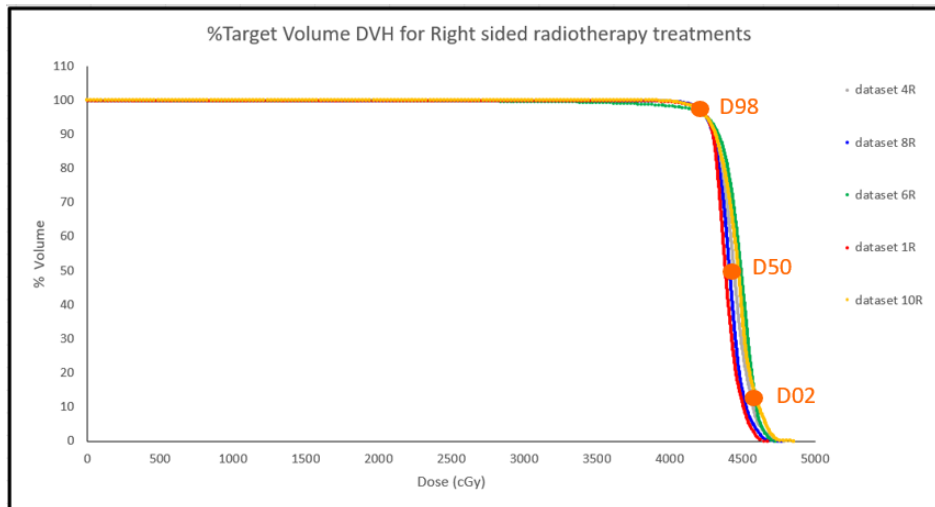


Figure 3-8: DVH curves for all right sided radiotherapy treatment sites.

Figure 3-7 and Figure 3-8 show the dose volume histograms with laterality separated to increase clarity. The purpose is to make clear the comparison with HI because the same information is contained in the DVH as in HI. The values that make up the HI have been added to Figure 3-8 for the benefit of the reader. The theory behind the homogeneity index is that the Ideal DVH will make a perfect square with the graph axis, meaning that a perfect distribution would have $D_{02\%}=D_{50\%}=D_{98\%}$ and the entire volume would absorb the same dose; here the HI would reach zero. In the opposite extreme, the worst distribution the DVH would form the hypotenuse of a right triangle with the axis being the legs, $D_{02\%}-D_{98\%}\approx D_{02\%}$ and the HI would be greater than 2.5 [16]. It is better to have an HI that is closer to zero, also the HI is not affected by dose level. Which means this plan quality metric is resistant to normalization. Because the HI of the SAP radiation distributions is equivalent to that of published literature, we can say that the radiation distribution is equivalently homogeneous overall, however the average D_{\max} values are higher and the average D_{mean} values are lower. This could indicate a lower, more homogeneous overall distribution which is offset by smaller high dose regions which achieve higher absorbed doses than what is present in published literature.

One possibility for this discrepancy is that the SAP at UTMC is less effective at rejecting bad segments. Currently the script is designed to close MLCs that are less than 1 cm apart to avoid long, thin control-points, however this has the un-intended side effect of also closing thinner portions of good segments, which may reduce overall field homogeneity. It has been proposed that the appropriate solution is to just segment quality by overall aperture open field area. This would add a human-like tool into the toolkit of SAP.

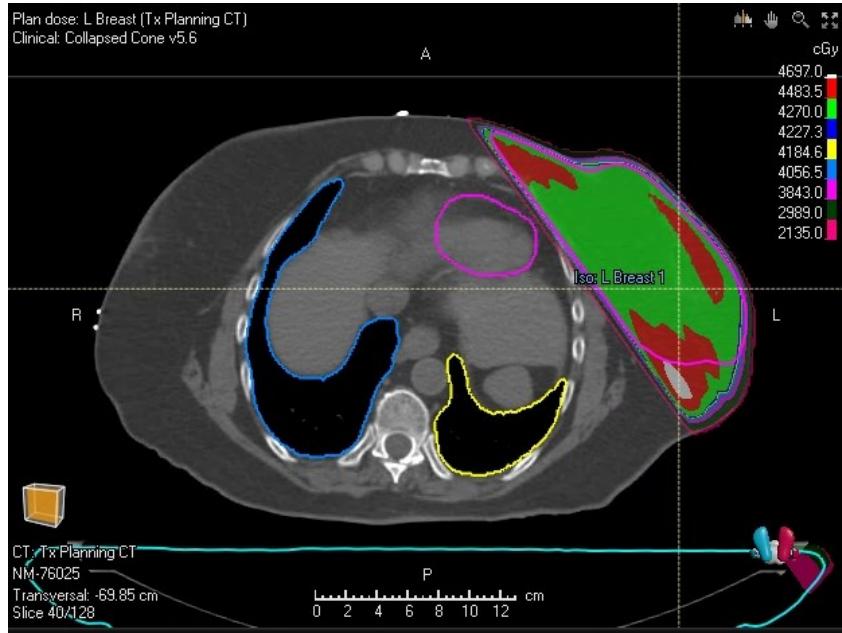


Figure 3-9: SAP developed radiation distribution for a left breast plan.

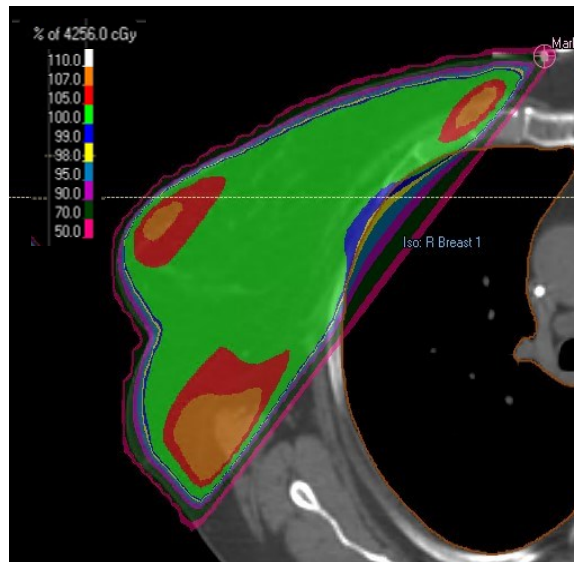


Figure 3-10: SAP developed radiation distribution for a right breast plan.

3.4 Automation grade

Table 3-4: Table of automation grade by dataset.

Dataset	Rx	RTOG passing normalization	Automation grade
dataset 1R	4256cGy/16 Fx	D95/V95	3
dataset 2L	4256cGy/16 Fx	D100/V95	3
dataset 3L	4256cGy/16 Fx	D100/V95	2
dataset 4R	4256cGy/16 Fx	D100/V95	1
dataset 5L	4256cGy/16 Fx	D100/V95	3
dataset 6R	4256cGy/16 Fx	D100/V95	3
dataset 7L	4256cGy/16 Fx	D100/V95	1
dataset 8R	4256cGy/16 Fx	D95/V95	1
dataset 9L	4256cGy/16 Fx	D100/V95	2
dataset 10R	4256cGy/16 Fx	D100/V95	4
Average	--	--	2.3

The judgement as to what makes a clinically acceptable dose distribution sometimes depends on the planner and the tradeoffs in organ dose that they are willing to make. However, it is prudent to maintain a standardized system to track the overall ability of automated software to produce a clinically usable outcome. This can be used in later work to track improvements to the software. Efforts should be made to improve the specificity of the automation grading system to a protocol that can be followed by the end user. Requiring an automation grade to be assigned to an auto-generated plan also provides an important opportunity to remind the end user to critically evaluate the quality

of the resultant dose distribution. Table 3-4 shows the automation grade for each plan generated, using a distinct variation on the automation grading system proposed in Heeren et al., based on a grade of 1 being clinically acceptable and 5 being not clinically usable.

Chapter 4

Conclusions

Breast cancer is the most common cancer in women [18]. Nearly 50 years of research has consistently shown radiotherapy treatment to be as effective at treating breast cancer as other therapies such as mastectomy [4] [19] [3]. With a successful history of long-term survival, radiotherapy will continue to be in demand as a breast cancer treatment. This means that the burden of treatment planning will also continue to cost the time of our healthcare professionals.

The question remains: what is the best use of the radiotherapy planners time and talents? They should be maximizing their time, concentrating on solving planning problems that the computer cannot solve. The job of the planner should be maximizing patient benefit. Automation techniques such as the SAP (Script Automated Planner) offer a method for creating segments and weightings that at least match the expectations of the Phase-3 trials that supply data on patient outcomes such as fast, fast-forward, and RTOG-1005 [4] [19] [20] [10]. While these plans will not produce the “perfect” plan on every patient geometry, the segments are made and can be easily tweaked and edited. This

times savings allows for rapid “plan prototyping” which and run in the background while the planner attends to other matters.

The SAP successfully created control points which compensate for the lack of tissue in the tissue regions which are distal to the patient. This was accomplished by interrogating the open field “Block” dose distribution with beam-direction specific isodose lines which mark dose gradients which must be compensated against. The plan, with optimized beam weightings then deletes under-used beams and closes unacceptably small control points, this can detriment the system if a segment aperture completely closes.

Dose distributions produced by the SAP have a most probably HI of 0.10, which is on par with previous studies [15]. The homogeneity is assessed at the standard clinical trial normalization of $D_{95\%}=95\%$ at which no volume received 107% dose. The dose distribution was also evaluated at the UTMC standard of $D_{95\%}=100\%$. Dose to OARs is mainly controlled via the initial human design of blocks and therefore do not factor into the main function of the SAP. However, only two plans out of ten had 20% of their lung volume reach 20% of the prescribed dose. Mean heart dose average 37 ± 6.5 cGy for Right breast plans and $80 \text{ cGy} \pm 2.79$ for left breasted plans. These dose statistics are not significant.

It becomes apparent that there is still room to improve the method by which SAP creates control points. A dose gradient also exists parallel to the beam direction which is not adequately accounted for in the final two to three control points, causing over coverage. Future work will include fine tuning the segmentation engine of SAP, while also controlling for minimum aperture size and shape. The small size of the dataset decreased the significance of the results, further study should be performed on an adequately sized data set to encompass most target volumes and geometries.

The final stage of the development cycle should include clinical acceptance testing which will inform the development of a strategy for quality management of auto-generated segmentation, to ensure a consistent quality of plan despite the lack of human beam segmentation and weighting.

The principles that undergird the segmentation engine of the SAP are generalizable to N beam directions, but are hindered by limits on MLC jaw travel, and therefore target size. This research has uncovered no other signs that the home-built SAP cannot be generalized to many sites with little to no effort.

Chapter 5

Future work

The script auto-planner is still in the development stages of its development and is not clinically accepted. It has not been used on patients in prospective or retrospective research or clinical use. It has been tested on a training atlas of CT datasets, only some of which may have originated from a breast treatment. Future research will require an approved application by the institutional review board. This however will provide a significant research benefit, allowing for testing in a broad range of different scenarios, this will also allow for comparison between the human generated dose distribution and the auto-generated plan, providing sufficient data for more complex and useful statistics.

Further research could include a generalization of the script automated protocol to other forms of 3D-CRT including sites such as whole brain, pelvis, spine, and extremities. There is no reason why other sites can't use the same method of interrogating the open field distribution with isodose lines. The SAP was written in such a way that the code will create segments based on dose gradients for N number of beams in the Blocks. An increase in beams and directions generally increases conformality of the dose

distribution. The script lays the foundation for the script automation of many 3D-CRT plans, and therefore has the potential to save planning staff a large amount of time.

Furthermore, the effectiveness of the SAP could be increased with the addition of more “human-like” functionality, such as sectioning off the thickest part of the breast, centered on the isocenter with an additional dummy beam and isodose ROI algebra which can be used to optimize beam weighting to reduce hotspot bridging across the medial portion of the target volume. One addition that is in the process of being added is the functionality to reject poor segments.

References

- [1] International Agency for Research on Cancer, World Cancer Report 2014, Lyon, France: World Health Organization, 2014.
- [2] A. N. Giaquinto, H. Sung, K. D. Miller, J. L. Kramer, L. A. Newman, A. Minihan, A. Jemal, R. L. Siegel and R. L. Siegel, Breast cancer statistics, 2022, CA: A Cancer J Clin, 2022.
- [3] B. Fisher, J. H. Jeong, S. Anderson, J. Bryant, E. R. Fisher and N. Wolmark, "Twenty-five-year follow-up of a randomized trial comparing radical mastectomy, total mastectomy, and total mastectomy following irradiation," *N Engl J Med*, vol. 347, no. 8, pp. 567-575, 2002.
- [4] B. A. Murray, J. S. Haviland, D. A. Wheatley, M. A. Sydenham, A. Alhasso, D. J. Bloomfield, C. Chan, M. Churn, S. Cleator, C. E. Cole, A. Goodman, A. Harnett, P. Hopwood, A. M. Kirby, C. C. Kirwan, C. Morris, Nabi Z, E. Sawyer, N. Somaiah, L. Stones, I. Syndikus, Bliss and J. R. Yarnold, "Hypofractionated breast radiotherapy for 1 week versus 3 weeks (Fast-forward): 5-year efficacy and late normal tissue effects results from a multicentre, non-inferiority, randomised, phase 3 trial," *Lancet*, vol. 395, no. 10237, pp. 1613-1626, 2020.
- [5] K. Rastogi, S. Sharma, S. Gupta, N. Agarwal, S. Bhaskar and S. Jain, "Dosimetric comparison of IMRT versus 3DCRT for post-mastectomy chest wall irradiation," *Radiat Oncol J*, vol. 36, no. 1, pp. 71-78, 2018.

- [6] S. Vivekandandan, J. Mhlanga, D. Launders, A. Przeslak and D. A. Morgan, "Beam angle manipulation to reduce cardiac dose during breast radiotherapy," *Br J Radiol*, vol. 85, no. 1011, pp. 265-271, 2012.
- [7] Á. K. P. S. Z. e. a. Gulybán, "Multisegmented Tangential Breast Fields: a Rational Way to Treat Breast Cancer," *Strahlenther Onkol*, vol. 184, pp. 262-269, 2008.
- [8] M. Sydenham, "Fast final protocol version 5, 30 July 2009 MREC approved - ICR.AC.UK. Prospective randomised clinical trial testing 5.7 Gy and 6.0 Gy fractions of whole breast radiotherapy in terms of late normal tissue responses and tumour control .," <https://www.icr.ac.uk/media/docs/default-source/clinical-trials/fast-final-protocol-version-5-30-july-2009-mrec-approved.pdf>, London, 2009.
- [9] F. A. Vicini, G. M. Freedman, J. R. White, M. Halyard, J. B. Owen, B. Rosenstein, S. M. Bentzen, X. Allen Li, R. J. Bleicher and K. Winter, "A Phase III Trial of Accelerated Whole Breast Irradiation with Hypofractionation Plus concurrent boost versus standard whole breast irradiation plus sequential boost for early-stage breast cancer," Radiation Therapy Oncology Group of the American College of Radiology, Philadelphia, PA, 2011.
- [10] F. A. Vicini, K. Winter, G. M. Freedman, D. W. Arthur, J. A. Hayman, B. S. Rosenstein, S. M. Bentzen, A. Li, J. Lyons, J. K. Tomberlin, S. a. Seaward, C. S, J. Coster, B. M. Anderson, F. E. Perera, M. M. Poppe, I. A. Peterson, J. Bazan Jr., J. Moughan and J. R. White, "NRG 1005: A Phase III Trial of Hypo Fractionated Whole Breast Irradiation with Concurrent Boost Versus conventional Whole Breast Irradiation Plus sequential boost following Lumpectomy for High Risk Early-stage Breast Cancer," ASTRO, San Antonio Tx, 2022.
- [11] G. a. D. J. F. L. Van Rossum, "Python reference manual," Centrum voor Wiskunde en Informatica, Amsterdam, 1995.

- [12] B. Archibald-Heeren, M. Byrne, Y. Hu, G. Liu, N. Collett, M. Cai and Y. Wang, "Single Click automated breast planning with iterative optimization," *J Appl Clin Med Phys*, vol. 21, no. 11, pp. 88-97, 2020.
- [13] P. R. Almond, P. J. Biggs, B. M. Coursey, W. F. Hanson, M. S. Huq, R. Nath and D. Rogers, "AAPM's TG-51 protocol for clinical reference dosimetry of high-energy photon and electron beams," *Med Phys*, vol. 26, pp. 1847-1870, 1999.
- [14] K. Huang, S. Hernandez, C. Wang, C. Nguyen, T. M. Briere, C. Cardenas, L. Court and Y. Xiao, "Automated field-in-field whole brain radiotherapy planning," *Journal of applied clinical medical physics*, vol. 24, p. e13819, 2023.
- [15] R. A. Mitchell, P. Wai, R. Colgan, A. M. Kirby and E. M. Donovan, "Improving the efficiency of breast radiotherapy treatment planning using a semi-automated approach," *J Appl Clin Med Phys*, vol. 18, pp. 18-24, 2017.
- [16] T. Kataria, K. Sharma, V. Subramani, K. P. Karrthick and S. S. Bisht, "Homogeneity Index: An objective tool for assessment of conformal radiation treatments," *Med Phys*, vol. 37, no. 4, pp. 207-213, 2012.
- [17] U. Blom Goldman, M. Anderson, B. Wennberg and P. Lind, "Radiation pneumonitis and pulmonary function with lung dose-volume constraints in breast cancer irradiation," *J Radiother Pract*, vol. 13, no. 2, pp. 211-217, 2014.
- [18] R. L. Siegel, K. D. Miller, N. S. Wagle and A. Jemal, "Cancer Statistics," *CA Cancer J Clin*, vol. 73, no. 1, pp. 17-48, 2023.
- [19] S. Darby, P. McGale, S. Correa, C. Taylor, R. Arrigada, M. Clark, Cutter D, C. Davies, M. Ewertz, J. Godwin, R. Gray, L. Pierce, T. Whelan, Y. Wang and R. Peto, "Effect of radiotherapy after breast-conserving surgery on 10-year recurrence and 15-year breast cancer death: meta-analysis of individual patient data for 10,801 women in 17 randomised trials," *Lancet*, vol. 378, no. 9804, pp. 1707-1716, 2011.

- [20] G. M. Freedman, J. R. White, D. W. Arthur, X. Allen Li and F. A. Vicini,
"Accelerated fractionation with a concurrent boost for early stage breast cancer,"
Radiother Oncol, vol. 106, no. 1, pp. 15-20, 2013.

Appendix A

Table A-1: Max point dose for left sided breast plans.

Left Breast: Max Point dose (% of Rx)		
Plan	D _{95%} =100%	D _{95%} =100%
Dataset 3L	108.9	105.0
Dataset 7L	107.5	102.1
Dataset 5L	111.8	105.2
Dataset 9L	111.9	106.3
Dataset 2L	108.7	103.3
mean	109.8	104.4
S.D.	1.993501179	1.648352316
constraint	Ideal	Adequate
RTOG Max point dose*	115	120
Not acceptable		

Table A-2: Max point dose for right sided plans.

Right Breast: Max Point dose (% of Rx)		
Plan	D _{95%} =100%	D _{95%} =95%
Dataset 4R	112.4	106.8
Dataset 8R	112.0	106.4
Dataset 6R	111.0	105.5
Dataset 10R	114.1	108.4
Dataset 1R	111.9	104.2
mean	112.3	106.3
S.D.	1.120801	1.555695056
constraint	Ideal	Adequate
RTOG Max point dose*	115	120
Not acceptable		

Table A-3: Mean Heart dose for left sided plans.

Left Breast: Mean Heart dose (cGy)		
Plan	D _{95%} =100%	D _{95%} =95%
Dataset 3L	84.11	80.67
Dataset 7L	78.94	75.01
Dataset 5L	76.6	72.93
Dataset 9L	80.43	76.34
Dataset 2L	78.67	74.76
Mean	79.75	75.942
S.D.	2.793608777	2.909049673
constraint	Ideal	Adequate
RTOG Maximum Mean heart dose*	400	500

Table A-4: Mean heart dose for right sided breast plans.

Right Breast: Mean Heart dose (cGy)		
Plan	D _{95%} =100%	D _{95%} =95%
Dataset 4R	44.72	42.51
Dataset 8R	34.39	32.68
Dataset 6R	44	41.82
Dataset 10R	31.5	29.93
Dataset 1R	32.1	30.52
Mean	37.342	35.492
S.D.	6.501647484	6.181825782
constraint	Ideal	Adequate
RTOG Maximum Mean heart dose*	400	500

Table A-5: Volume of heart receiving 20 Gy in left sided breast plans

Left Breast: Heart V _{20 Gy} (in % Volume)		
Plan	D _{95%} =100%	D _{95%} =95%
Dataset 3L	0	0
Dataset 7L	0	0
Dataset 5L	0.01	0.01
Dataset 9L	0	0
Dataset 2L	0	0
Mean	0.002	0.002
S.D.	0.004472136	0.004472136
constraint	Ideal	Adequate
RTOG Max volume at dose*	20 Gy	25 Gy

Table A-6: Volume of heart receiving 20 Gy in right sided breast plans

Right Breast: Heart V _{20 Gy} (in % Volume)		
Plan	D _{95%} =100%	D _{95%} =95%
Dataset 4R	0	0
Dataset 8R	0	0
Dataset 6R	0	0
Dataset 10R	0	0
Dataset 1R	0	0
Mean	0	0
S.D.	0	0
constraint	Ideal	Adequate
RTOG Max volume at dose*	20 Gy	25 Gy

Table A-7: Volume of heart receiving 10 Gy in left sided breast plans.

Left Breast: Heart V _{10 Gy} (in % Volume)		
Plan	D _{95%} =100%	D _{95%} =95%
Dataset 3L	0	0
Dataset 7L	0	0
Dataset 5L	0.01	0.01
Dataset 9L	0.01	0.01
Dataset 1L	0	0
Mean	0.004	0.004
S.D.	0.005477226	0.005477226
RTOG Max volume at dose*	Ideal	Adequate
	< 30%	< 35%

Table A-8: Volume of heart receiving 10 Gy in Right sided breast plans

Right Breast: Heart V _{10 Gy} (in % Volume)		
Plan	D _{95%} =100%	D _{95%} =95%
Dataset 4R	0	0
Dataset 8R	0	0
Dataset 6R	0	0
Dataset 10R	0	0
Dataset 1R	0	0
Mean	0	0
S.D.	0	0
RTOG Max volume at dose*	Ideal	Adequate
	< 30%	< 35%

Table A-9: Max point dose to the Contralateral –Right—Breast in Left sided breast plans.

Left Breast: Contralateral Breast Maximum Point dose (cGy)		
Plan	D _{95%} =100%	D _{95%} =95%
Dataset 4R	210.41	201.87
Dataset 8R	257.94	245.03
Dataset 6R	74.17	67.97
Dataset 10R	228.05	216.62
Dataset 1R	351.58	334.15
Mean	224.43	213.128
S.D.	100.0971715	96.01281644
RTOG Max point dose*	Ideal	Adequate
	300	330
Not acceptable		

Table A-10: Max point dose to the Contralateral –Left—Breast in Right sided breast plans.

Right Breast: Contralateral Breast Maximum Point dose (cGy)		
Plan	D _{95%} =100%	D _{95%} =95%
Dataset 4R	518.93	493.09
Dataset 8R	264.62	251.54
Dataset 6R	253.3	240.7
Dataset 10R	245.93	233.74
Dataset 1R	291.62	278.1
Mean	314.88	299.434
S.D.	115.3794789	109.5639146
RTOG Max point dose*	Ideal	Adequate
	300	330
Not acceptable		

Table A-11: Volume at dose statistics for Ipsilateral –left-- Lung in left sided breast plans.

Left Breast: Ipsilateral --Left-- Lung (Volume % of contour)			
Plan: D _{95%} =100%	V _{20Gy}	V _{10Gy}	V _{5Gy}
Dataset 3L	2	5	10
Dataset 7L	14	17	23
Dataset 5L	9	11	15
Dataset 9L	18	23	31
Dataset 2L	7	11	16
mean	10	13	19
S.D.	6.204836823	6.841052551	8.154753
RTOG Volume at dose: ideal	15	35	50
RTOG Volume at dose: acceptable	20	40	50
Not acceptable			

Table A-12: Volume at dose statistics for Ipsilateral –Right-- Lung in Right sided breast plans.

Right Breast: Ipsilateral --Right-- Lung (Volume % of contour)			
Plan: D _{95%} =100%	V _{20Gy}	V _{10Gy}	V _{5Gy}
Dataset 4R	12	17	23
Dataset 8R	20	25	31
Dataset 6R	14	18	24
Dataset 10R	14	19	27
Dataset 1R	9	12	17
mean	14	18	24
S.D.	4.024922359	4.65832588	5.176872
RTOG Volume at dose: ideal	15	35	50
RTOG Volume at dose: acceptable	20	40	50
Not acceptable			

Table A-13: Volume at dose tables for Ipsilateral –left–Lung in left sided breast plans when normalized to the literature standard of $D_{95\%}=95\%$.

Left Breast: Ipsilateral --Left-- Lung (Volume % of contour)			
Plan: $D_{95\%}=95\%$	V_{20Gy}	V_{10Gy}	V_{5Gy}
Dataset 3L	2	4	9
Dataset 7L	13	17	23
Dataset 5L	8	11	14
Dataset 9L	18	23	30
Dataset 2L	7	10	15
mean	10	13	18
	6.107372594	7.245688373	8.288546
RTOG Volume at dose: ideal	15	35	50
RTOG Volume at dose: acceptable	20	40	50
Not acceptable			

Table A-14: Volume at dose tables for Ipsilateral –left–Lung in left sided breast plans when normalized to the literature standard of $D_{95\%}=95\%$.

Right Breast: Ipsilateral --Right-- Lung (Volume % of contour)			
Plan: $D_{95\%}=95\%$	V_{20Gy}	V_{10Gy}	V_{5Gy}
Dataset 4R	12	16	23
Dataset 8R	20	24	31
Dataset 5L	13	18	23
Dataset 9L	14	19	26
Dataset 1R	9	12	17
mean	14	18	24
	4.037325848	4.38178046	5.09902
RTOG Volume at dose: ideal	15	35	50
RTOG Volume at dose: acceptable	20	40	50
Not acceptable			

Table A-15: Proportion of each dataset that received dose of 103%, 105%, and 107% for plans normalized to $D_{95\%}=95\%$.

Proportion of PTV at Dose Levels above Rx ($D_{95\%}=95\%$)			
Dataset	103%	105%	107%
dataset 1R	0.01	0	0
dataset 2L	0.00305	0	0
dataset 3L	0.00305	0	0
dataset 4R	0.025	0.00175	0
dataset 5L	0.015	0	0
dataset 6R	0.065	0.005	0
dataset 7L	0.01	0	0
dataset 8R	0.025	0.00175	0
dataset 9L	0.115	0.00818	0
dataset 10R	0.18	0.02	0
Average (%)	4.511	0.3668	0
S.D. (%)	1.3051031	1.732601693	0

Table A-16: Proportion of each dataset that received dose of 103%, 105%, and 107% for plans normalized to $D_{95\%}/V_{100\%}$.

Proportion of PTV at Dose Levels above Rx ($D_{95\%}=95\%$)			
Dataset	103%	105%	107%
dataset 1R	0.495	0.17	0.045
dataset 2L	0.74	0.32	0.025
dataset 3L	0.715	0.25	0.03695
dataset 4R	0.725	0	0
dataset 5L	0.835	0.835	0.835
dataset 6R	0.835	0.59	0.235
dataset 7L	0.49	0.045	0.08
dataset 8R	0.6419	0.23	0.07
dataset 9L	0.76	0.48	0.265
dataset 10R	0.785	0.53	0.195
Average (%)	70.219	34.5	17.8695
S.D. (%)	0.177096041	0.757761461	1.39179573

Table A-17: Homogeneity index values calculated using the $D_{50\%}$ as the denominator instead of the prescription.

Dataset	HI
dataset 1R	0.094
dataset 2L	0.080
dataset 3L	0.079
dataset 4R	0.107
dataset 5L	0.130
dataset 6R	0.132
dataset 7L	0.062
dataset 8R	0.098
dataset 9L	0.110
dataset 10R	0.118
Average	0.101
S.D.	0.022